



Regular Article

## Facile co-precursor sol-gel synthesis of a novel amine-modified silica aerogel for high efficiency carbon dioxide capture



Zai-Dong Shao <sup>a,b</sup>, Xuan Cheng <sup>c,d</sup>, Yu-Ming Zheng <sup>a,b,\*</sup>

<sup>a</sup> CAS Center for Excellence in Regional Atmospheric Environment, Institute of Urban Environment, Chinese Academy of Sciences, Xiamen, Fujian 361021, China

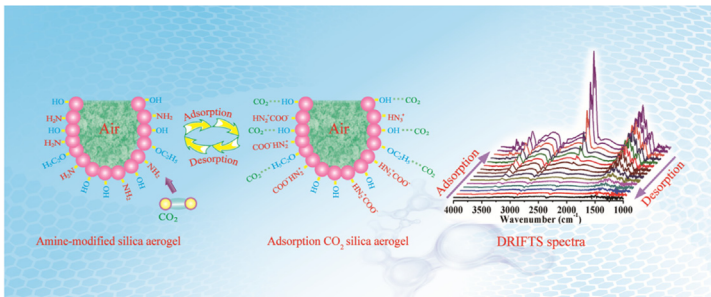
<sup>b</sup> CAS Key Laboratory of Urban Pollutant Conversion, Institute of Urban Environment, Chinese Academy of Sciences, Xiamen, Fujian 361021, China

<sup>c</sup> Department of Materials Science and Engineering, College of Materials, Xiamen University, Xiamen, Fujian 361005, China

<sup>d</sup> Fujian Key Laboratory of Advanced Materials, Xiamen, Fujian 361005, China

### GRAPHICAL ABSTRACT

Amine-modified silica aerogel fabricated by a rapid and simple co-precursor sol-gel procedure demonstrated high efficiency for CO<sub>2</sub> capture from flue gas.



### ARTICLE INFO

#### Article history:

Received 14 May 2018

Revised 28 June 2018

Accepted 28 June 2018

Available online 30 June 2018

#### Keywords:

Amine

Modification

Silica aerogel

Carbon dioxide

Adsorption

### ABSTRACT

Massive amount of CO<sub>2</sub> emission, which could cause climate change, has been recognized as a serious environmental issue. Chemical adsorption is generally considered as a promising technology for CO<sub>2</sub> capture in low CO<sub>2</sub> partial pressure. Physical properties and chemical components of the adsorbent are important to CO<sub>2</sub> adsorption performance. To address structure limitation and complicated preparation process of the conventional adsorbent, herein, we reported a rapid and simple route to synthesis amine-modified silica aerogel monolith by co-precursor sol-gel method. Microstructure and the surface functional groups of the amine-modified silica aerogel could be easily manipulated. The products were characterized by SEM, XPS, NMR, in situ DRIFT and CNS elemental analyzer. The amine-modified silica aerogel exhibited good physical properties and demonstrated excellent CO<sub>2</sub> adsorption performance. The density, porosity and BJH pore volume of the amine-modified silica aerogel were 0.12 g/cm<sup>3</sup>, 94.5% and 2.39 cm<sup>3</sup>/g, respectively. The maximum static and dynamic adsorption capacities of CO<sub>2</sub> on the amine-modified silica aerogel were 2.2 mmol/g and 5.59 mmol/g under anhydrous and humid mixed gas conditions, respectively. The as-prepared aerogel also showed good cyclic ability for CO<sub>2</sub> adsorption and desorption. The CO<sub>2</sub> adsorption on the amine-modified silica aerogel is by the formation of carbamate through a two-step zwitterion mechanism. This easily prepared amine-modified silica aerogel could be a promising adsorbent for CO<sub>2</sub> capture.

© 2018 Elsevier Inc. All rights reserved.

\* Corresponding author at: CAS Center for Excellence in Regional Atmospheric Environment, Institute of Urban Environment, Chinese Academy of Sciences, Xiamen, Fujian 361021, China.

E-mail address: [ymzheng@iue.ac.cn](mailto:ymzheng@iue.ac.cn) (Y.-M. Zheng).

## 1. Introduction

Greenhouse gas (GHG) emission has been recognized as a potential risk to climate change and natural ecosystem health. Especially, the disadvantaged people and communities all over the world will suffer bigger risks from the emission of massive amount of greenhouse gas [1]. Carbon dioxide ( $\text{CO}_2$ ) emission, making up about 60% of the global GHG, usually comes from combustion of fossil fuels and is currently recognized as the dominant contributor to global warming [2,3]. The anthropogenic  $\text{CO}_2$  emission mainly originates from the flue gases with  $\text{CO}_2$  concentrations ranging from 10% to 15%. Hence,  $\text{CO}_2$  capture, sequestration and utilization is considered as an energy-efficient and promising way to mitigate the risks of massive  $\text{CO}_2$  emission [4]. Various methods, such as liquid adsorption, solid physical/chemical adsorption, membrane separation and biotechnology, have been proposed for capturing  $\text{CO}_2$  from the atmosphere [5–9]. Among the above-mentioned methods, adsorptive separation by organic functionalized porous materials is often regarded as the most simple and effective technique for  $\text{CO}_2$  capture. Therefore, much attention has been paid to develop  $\text{CO}_2$  adsorbent with high adsorption capacities and excellent adsorption selectivity for potential practical applications.

Compared with physical adsorbents, such as activated carbons, micro-porous zeolites and metal organic frameworks, chemical adsorbents often showed better adsorption performance, thus, have attracted more attentions [10–12]. One of the common way for developing chemical adsorbent for  $\text{CO}_2$  capture is to graft amine groups onto the surface of porous materials, such as mesoporous silica [13–16]. Amine-modified porous silicas have exhibited unique properties, such as high adsorption selectivity towards  $\text{CO}_2$  (especially in low partial pressure), enhancement of  $\text{CO}_2$  adsorption capacities in the presence of moisture, good cyclic stability, and wide range of temperature applicability [15]. For example, the amine-functionalized mesoporous silica prepared by surfactant-mediated synthesis demonstrated a low  $\text{CO}_2$  adsorption capacity of 1.247 mmol/g, and 6.7% drop in the adsorption capacity after ten cycles of  $\text{CO}_2$  adsorption-desorption [16].

It is considered that the physical properties of porous supporting materials for amine-functionalized carbon dioxide adsorbent are closely related to its  $\text{CO}_2$  adsorption performance. Because of its unique and excellent physical properties, mesoporous silica aerogel has been recognized as a wonderful porous support for amine modification, which can be subsequently used as  $\text{CO}_2$  adsorbent. Silica aerogel is a kind of three-dimensional nanoporous material with low density (0.003–0.35 g/cm<sup>3</sup>) and high porosity (88–99.8%), which possess extraordinary properties, including large specific surface area (600–1500 m<sup>2</sup>/g), high optic transmission (>60%) and potential applications in many fields [17–21]. However, the dominant surface functional groups of pure silica aerogel are hydrophilic Si-OH groups or hydrophobic Si-CH<sub>3</sub> groups depending on the drying method, which should be modified to improve  $\text{CO}_2$  adsorption performance.

To prepare high performance  $\text{CO}_2$  adsorbent, it is important to graft amine functional groups on the silica aerogel network without damaging the physical properties of silica aerogel. Most of the reported amine-modified silica aerogels used as  $\text{CO}_2$  adsorbent were usually prepared by a two-step method, that is synthesis of pure silica aerogel followed by post amine-modification via grafting. However, this method usually leads to the unevenly distribution and hardly precise control of amine group content. Even worse, the amine silane often blocks the pores of silica aerogel. For example, the amine-modified silica aerogel could be prepared by immersing pure silica wet-gel into 3-aminopropyltriethoxysilane (APTES)/ethanol solution, the APTES diffuses into the gel by

capillary force and then grafts to the surface of gel network by the condensation reaction with Si-OH groups. It was shown that the  $\text{CO}_2$  adsorption capacity of the amine-modified silica aerogel was only 2.0 mmol/g at 298 K, indicating the grafted amine species could damage to the physicochemical properties of the aerogel, so a low  $\text{CO}_2$  adsorption capacity of the modified aerogel was obtained [22]. Similar procedures were reported for grafting mono, di and tri-amine silanes to the silica aerogel [23].

Anionic surfactant template and sol-gel co-precursor methods are another two types of traditional method of fabricating amine-modified silica aerogel [16]. For anionic surfactant template method, the amines are directly incorporated into the silica matrix mediated by surfactant. However, the introduced surfactant is hard to be completely removed from the porous silica, which would damage to the pore of the as-made porous silica during drying process.

Co-precursor method is an in-situ and one-step procedure to fabricate organo-functionalized silica network. The growth mechanism and microstructure of the obtained silica network is controlled by the sol-gel process. The growth of silica network could be tailored by two different mechanisms, reaction limited cluster aggregation (RLCA) and reaction limited monomer cluster growth (RLMC). Many types of organo-functionalized silica aerogels with good physical properties could be synthesized through the RLCA growth mechanism, such as epoxy, isocyanato, methyl, and vinyl modified silica aerogel [24–26]. Generally, in the RLCA growth mechanism, the silica gel is prepared by hydrolysis and condensation reactions of silica source as follows, first, organic silanes and silica precursor hydrolyze to form independent solid colloidal particles. Then, the base catalysts play as proton acceptors to accelerate the condensation reactions, in which the colloidal particles are condensed and link with each other to build a three-dimensional gel network structure.

However, it is difficult to synthesize amine-modified silica aerogel with good physical properties by the RLCA growth mechanism. The reason is that the co-precursor of amine silane plays dual roles of both modification agent and base catalyst during the sol-gel processing. The existence of amine silane will increase the pH of the silica sol to be basic. Under basic condition, RLMC mechanism will be involved in the silica network growth progress, during which the hydrolysis reaction of silica alkoxysilane becomes the rate-determining step, and the small amount of hydrolyzed Si-OH groups are immediately consumed because of the faster condensation reaction, which results in a precipitation of denser silica particles instead of gelation of fragile silica network. The prepared silica gel network is also easy to be destroyed during the drying process. Furthermore, the preparation of amine-modified silica aerogel by co-precursor method with RLMC growth mechanism required long time and multiple stages of solvent exchange before drying, and aerogels with poor physical properties were obtained [27].

To overcome the above mentioned drawbacks, copolymerization of tetramethylorthosilicate (TMOS)/APTES have been developed to fabricate the amine-modified silica wet-gel, which should be cooled down to -78 °C in a dry ice-acetone bath in order to slow down the condensation reaction of silanes [28]. Hence, the existing methods of fabrication of amine-modified aerogel require rigorous and complicated procedure.

In this paper, we developed a novel rapid and simple co-precursor sol-gel procedure, with no requirement of solvent exchange, for the fabrication of novel transparent amine-modified silica aerogels, which demonstrated to be a highly efficient  $\text{CO}_2$  adsorbent. The amine-modified silica gel network was constructed based on the RLCA mechanism. The sol-gel process of silica aerogel fabrication was manipulated by the rate of

hydrolysis and condensation reaction, which was regulated by the reaction temperature and silica source groups. The highly porous nano-skeleton and chemical components of the modified silica aerogel could be easily controlled. The as-fabricated amine-functionalized silica aerogel showed excellent physical properties and high CO<sub>2</sub> adsorption performance, which were much better than those of the reported amine-modified porous silicas in the literature. The process and mechanism of CO<sub>2</sub> adsorption on the amine-modified silica aerogel were also investigated in-depth.

## 2. Experimental

### 2.1. Chemicals

Tetraethoxysilane (TEOS) ( $\geq 98.0\%$ ) and ethanol ( $\geq 99.7\%$ ) were obtained from Sinopharm Chemical Reagent Co. Ltd., China. 3-Aminopropyltriethoxysilane (APTES) ( $\geq 99.0\%$ ) was purchased from Aladdin Chemical Reagent Co. Ltd, China.

### 2.2. Preparation of the amine-modified silica aerogel

APTES solution with APTES:EtOH:H<sub>2</sub>O molar ratio of 1:13.5:12 was prepared, followed by continuous agitation for 12 h. Then, TEOS was directly added into the hydrolyzed APTES solution at a APTES/TEOS molar ratio of 1:2. The formed silica sol was kept in a refrigerator at  $-18^{\circ}\text{C}$  until the gelation of silica sol was completed. The silica wet-gel was aged at  $55^{\circ}\text{C}$  for 6 h to allow the strengthening of gel network. Finally, the aged silica wet-gel was directly dried by CO<sub>2</sub> supercritical drying to prepare amine-modified silica aerogel. In contrast, the amine-modified silica xerogel was dried at  $80^{\circ}\text{C}$  for 2 h, the pure silica aerogel was prepared with the molar ratio of TEOS:EtOH:H<sub>2</sub>O of 1:7:6 and followed by aging and supercritical drying.

### 2.3. Characterization of the amine-modified silica aerogel

The specific surface area, pore volume and pore size distribution of pure silica aerogel and amine-modified silica xerogel/aerogel were estimated by nitrogen adsorption-desorption isotherm analysis with a surface area and porosity analyzer (ASAP2020M+C, Micromeritics). The surface and cross-sectional morphology of pure silica aerogel and amine-modified silica xerogel/aerogel was examined by field emission scanning electron microscope (FESEM, Hitachi S-4800, Japan). The element content of carbon and nitrogen were tested by CNS elemental analyzer (Vario MAX, Germany). Thermal stability of amine-modified silica aerogel was studied by thermo gravimetric analysis (TG209F1, NetzschTartus, Germany). The crystal structure of pure silica aerogel and amine-modified silica xerogel/aerogel was analyzed using an X-ray diffractometer (XPert PRO, Philips, Netherlands) with Cu Ka ( $\lambda = 0.1542 \text{ nm}$ ) radiation. The <sup>29</sup>Si and <sup>13</sup>C solid-state magic angle spinning nuclear magnetic resonance (MAS NMR) spectra were collected on a spectrometer (Advance III, Bruker) at 400 MHz. The XPS spectra were recorded on Scanning ESCA Microprobe using Al Ka radiation (Quantum2000, PHI). The quantitative XPS analysis was performed by multiple-curve fitting of each elemental spectrum, and the amount of each species was calculated by the relative ratio of the corresponding integrated areas with the total integrated areas. The peak locations of all relevant species were determined based on previous works.

### 2.4. Static and dynamic adsorption of CO<sub>2</sub>

Static adsorption experiments and isotherm model analyses were performed to investigate the adsorption performance and surface characteristics of the adsorbent. The static adsorption of

CO<sub>2</sub> on the pure silica aerogel and the amine-modified silica xerogel/aerogel were investigated by a pore structure analyzer (Autosorb-iQ, Quantachrome). Prior to each measurement, the sample was pretreated at  $150^{\circ}\text{C}$  under vacuum for 6 h. The CO<sub>2</sub> adsorption experiments were performed at 273 K and 298 K, respectively. The temperature was controlled by a thermostatic circulating fluid.

In order to describe nature of the adsorbent, four commonly used adsorption isotherm models including Langmuir, Freundlich, Toth and Sips equations were formulated to fit the experimental adsorption data.

Langmuir isotherm model is given by Eq. (1):

$$q_e = q_m \frac{bP}{1 + bP} \quad (1)$$

where  $q_e$  (mmol/g),  $q_m$  (mmol/g) and  $b$  represent the equilibrium adsorption amount, the maximum monolayer adsorption capacity and the Langmuir constant related to adsorption energy, respectively.

Freundlich isotherm model is given by Eq. (2):

$$q_e = K_F P^{1/n} \quad (2)$$

where  $K_F$  (mmol/g) is the Freundlich constant related to adsorption capacity, and  $1/n$  is the heterogeneity factor describing the adsorption intensity.

Toth isotherm model is given by Eq. (3):

$$q_e = \frac{n_s bP}{(1 + (bP)^t)^{1/t}} \quad (3)$$

where  $n_s$  (mmol/g) and  $t$  represent the maximum adsorption capacity and the surface heterogeneity of the adsorbent, respectively.

Sips Equation is given by Eq. (4):

$$q_e = q_m \frac{(bP)^{1/n}}{1 + (bP)^{1/n}} \quad (4)$$

where  $q_m$  (mmol/g) and  $n$  are the maximum adsorption capacity and the measure of surface heterogeneity.

To describe the accuracy of the proposed isotherm models, error was calculated by an error function based on the normalized standard deviation by:

$$\Delta q(\%) = \sqrt{\frac{\sum [(q_{\text{exp}} - q_{\text{model}})/q_{\text{exp}}]^2}{N - 1}} \times 100 \quad (5)$$

In addition, the adsorption performance of CO<sub>2</sub> on the adsorbent was also evaluated by dynamic adsorption tests. The experiments of dynamic adsorption of CO<sub>2</sub> on the pure silica aerogel, amine-modified silica xerogel and aerogel were conducted in a quartz reactor. Prior to each test, the adsorbent was pretreated at  $150^{\circ}\text{C}$  under 100 ml/min of N<sub>2</sub> flow for 2 h. For CO<sub>2</sub> adsorption, CO<sub>2</sub>/N<sub>2</sub> mixed gas with 10% CO<sub>2</sub> was used, and the mixed gas flow rate was maintained at 30 ml/min by mass flow meter. Meanwhile, 1% water vapor was generated and introduced at a steady state. The dosage of adsorbent was 0.3 g, and the temperature of the tubular reactor was controlled in a tube furnace and varied in a range of 20–50 °C. CO<sub>2</sub> concentration in the gas outlet was measured using a gas chromatography (GC9790II, Fulí Analytical Instrument Co. Ltd., China) and the data were collected by a Data-Chart 3000 (Monarch Instrument Inc., Amherst, NH).

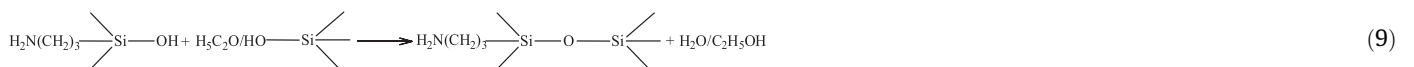
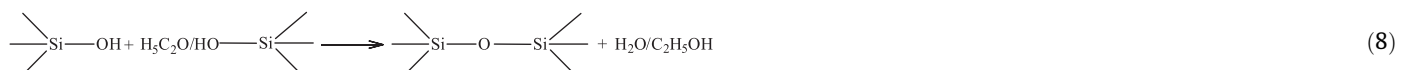
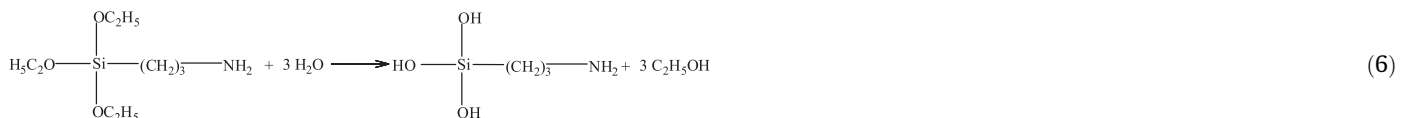
### 2.5. CO<sub>2</sub> adsorption and desorption mechanism analysis

The in-situ diffusion reflectance infrared Fourier transform spectroscopy (DRIFTS) setup was used for CO<sub>2</sub> adsorption and desorption study, which could provide insights into the mechanisms

of adsorption/desorption and mass transfer processes occurring on the amine-modified silica aerogel. The measurements were performed with ZnSe windows in a DRIFT cell and investigated by Fourier transform infrared spectrometer (FTIR, Nicolet iS50 Thermo-Nicolet). In CO<sub>2</sub> adsorption experiment, the amine-modified aerogel was pretreated at 150 °C in a 100 ml/min N<sub>2</sub> flow for 1 h and then cooled to 25 °C. The background spectrum was recorded in a pure N<sub>2</sub> flow, and then the spectrum of CO<sub>2</sub> adsorption was measured by switching the N<sub>2</sub> flow to a 2 ml/min CO<sub>2</sub> flow via a 3-port valve. In the CO<sub>2</sub> desorption experiment, the amine-modified aerogel saturated with CO<sub>2</sub> was treated in a 100 ml/min N<sub>2</sub> flow at 25 °C for 20 min. Then the experiment of CO<sub>2</sub> temperature programmed desorption was conducted by heating to 200 °C at 10 °C/min in 100 ml/min N<sub>2</sub> flow. The normalized IR absorbance intensity was calculated by  $I_t/I_{\max}$ , where  $I_t$  is the absorbance intensity at time t for profile of interest,  $I_{\max}$  is the maximum profile intensity.

the hydrolysate of APTES sol with silica precursor of TEOS. Next, the silica wet-gel network was formed by condensation, which led to the formation of silica secondary particles during the sol-gel process. Finally, the amine-modified silica aerogel was obtained by CO<sub>2</sub> supercritical drying to prevent the pore collapses due to the surface tension.

The chemical reactions during the sol-gel process can be formally expressed by the following reactions. APTES was hydrolyzed by water to convert Si-OCH<sub>2</sub>CH<sub>3</sub> to Si-OH through Reaction (6). When hydrolyzed APTES was mixed with TEOS, the hydrolysis (Reaction (7)) and condensation (Reactions (8) and (9)) occur simultaneously, and the presence of Si-ORx groups would decrease the relative condensation rate. The reaction temperature was controlled to minimize the difference between the rate of hydrolysis and condensation reaction. Hence, the preparation process of amine-modified silica gel network was similar to that of reaction limited cluster aggregation.



### 3. Results and discussion

#### 3.1. Synthesis of amine-modified silica aerogel

The synthetic route of the amine-modified silica aerogel was presented in Fig. 1. First, the silica sol was prepared by mixing

As shown in Fig. 2, the photograph of amine-modified silica aerogel monolith exhibited semi-transparent and no visible cracks, which suggested smaller clusters were formed and condensed to small silica particles during sol-gel process. The TG curves in Supplement Fig. S1 indicate over 30% weight loss up to 800 °C with the modified silica aerogel. The weight loss from 100 °C to 200 °C



**Fig. 1.** Schematic diagram of preparation of the amine-modified silica aerogel.

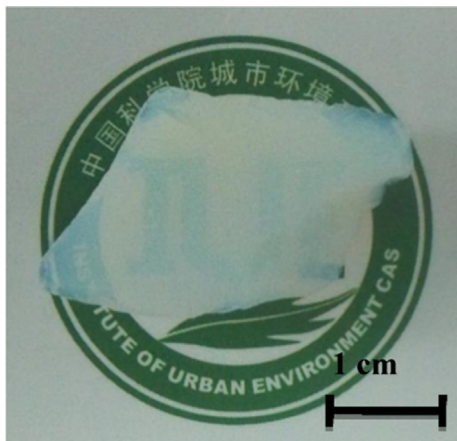
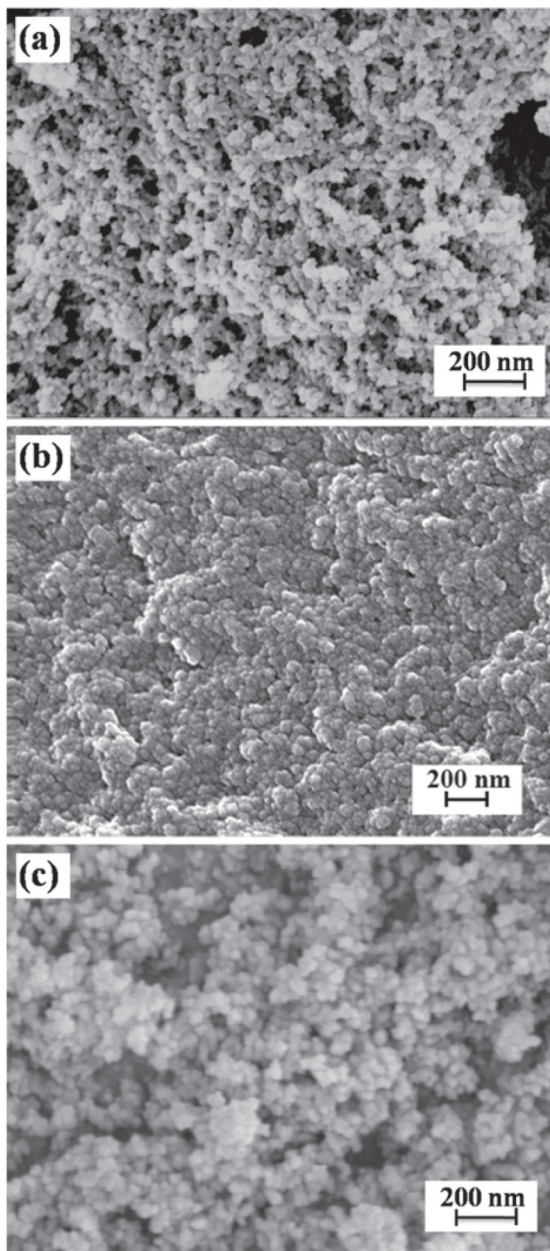


**Fig. 2.** Photograph of amine-modified silica aerogel.



corresponded to the release of the adsorbed water and ethanol on the silica network, the main loss at the temperature higher than 200 °C was assigned to the oxidation of modified amine group by APTES and little amount of incomplete hydrolysis of  $-\text{OCH}_2\text{CH}_3$ .

Supplementary data associated with this article can be found, in the online version, at <https://doi.org/10.1016/j.jcis.2018.06.094>.

### 3.2. Characterization of the amine-modified silica aerogel

The pure silica aerogel and amine-modified silica xerogel/aerogel demonstrate different surface morphologies as shown in Fig. 3a–c. The pure silica aerogel consists of aggregated silica nanoparticles and shows loose microstructure with a large amount of mesopores. The high porosity of aerogel was attributed to the nano-skeleton, which was maintained via supercritical drying. The amine-modified silica aerogel also showed a similar loose three-dimensional network compared to pure silica aerogel.

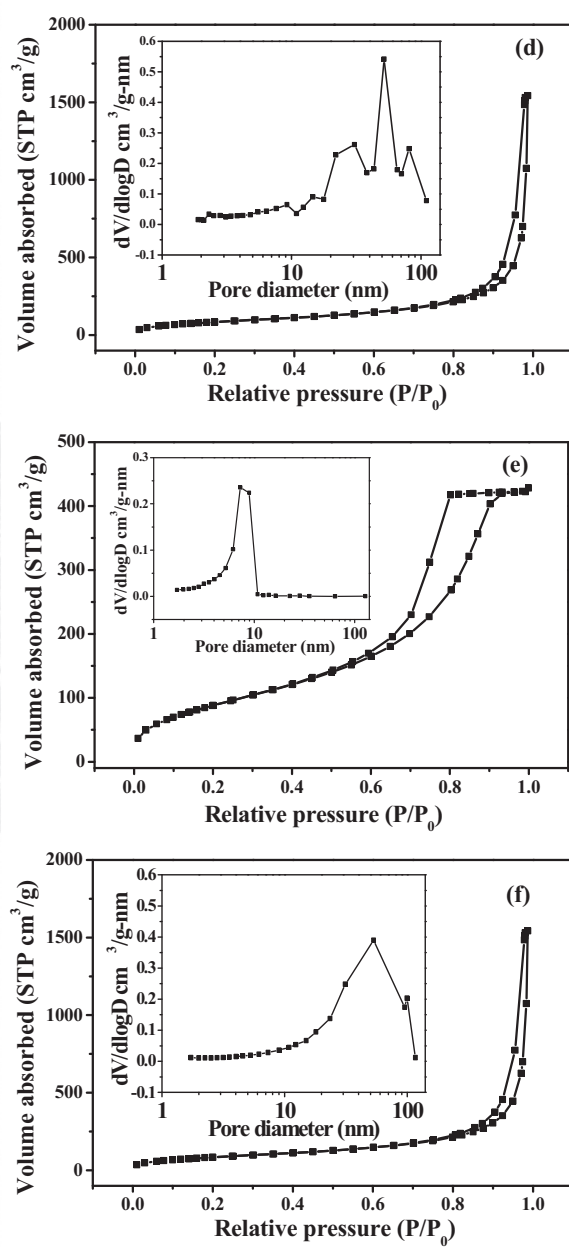


**Fig. 3.** SEM micrographs and nitrogen adsorption-desorption isotherms of pure silica aerogel (a, d), and amine-modified xerogel (b, e) and aerogel (c, f). The inserts show the corresponding pore size distribution curves.

However, the amine-modified silica xerogel showed dense silica nanoparticles and low porosity, which might be ascribed to collapsing of nano-skeleton via ambient pressure drying.

The nitrogen adsorption-desorption isotherms and pore size distribution curves of pure silica aerogel and amine-modified silica xerogel/aerogel are shown in Fig. 3. The isotherms for both pure and amine-modified silica aerogels displayed typical IV isotherms with type H<sub>3</sub> hysteresis loop, which indicates a characteristic distribution of slit-shaped pores. The pore size distribution curves also showed both the pure and amine-modified silica aerogels maintained high porous structure with the main pore size distribution of about 50 nm. The nitrogen adsorption isotherm for the amine-modified silica xerogel showed a typical type IV isotherm with H<sub>2</sub> hysteresis loop, indicating a characteristic distribution of ink bottle shaped pores. The isotherm type also indicated that the pore structure of silica wet-gel have seriously shrinkage and collapse during ambient pressure drying. The physical properties of samples are summarized in Table S1. The porous amine-modified silica aerogel showed a low density of about 0.12 g/cm<sup>3</sup> and a high BJH pore volume of 2.39 cm<sup>3</sup>/g, which were close to the physical properties of pure silica aerogel, suggesting the porous nanostructure was maintained. The higher porosity of aerogel could be contributed from the maintained nano-skeletons via supercritical drying. However, the BET specific surface area of amine-modified aerogel is 318 m<sup>2</sup>/g, which is obviously lower than the pure silica aerogel of 738.5 m<sup>2</sup>/g. The average pore size of amine-modified aerogel is 23.6 nm, which is quite different from that of pure silica aerogel of 11.2 nm. The average pore size and BJH pore volume of silica xerogel decreased to 6.0 nm and 0.67 cm<sup>3</sup>/g respectively, because of the volume shrinkage of silica xerogel during ambient pressure drying process.

The broad diffractions at 2θ values of ~22° were observed with the pure silica aerogel and amine-modified silica xerogel/aerogel in XRD patterns (Fig. S2 in the supplementary information), which are regarded as diffused type conforming more toward amorphous nature. Thus, amine modification caused insignificantly change in the network structure. However, surface chemical components of the amine-modified silica aerogels were noticeably changed due to the introducing amine as evident in Figs. 4 and S4.

As shown in Fig. S4, FTIR spectra of both the pure silica aerogel and the amine-modified silica aerogel demonstrated the typical Si-O-Si asymmetric, symmetric and rocking bending absorption peaks at the wavenumber of 1080, 800 and 450 cm<sup>-1</sup> respectively. For the amine-modified silica aerogel, a new absorption peak appeared at the wavenumber of 1580 cm<sup>-1</sup> which was caused by the

vibration of NH<sub>2</sub>, indicating successful modification of the silica aerogel by APTES. The solid state <sup>29</sup>Si and <sup>13</sup>C NMR spectra are presented in Fig. 4. Two obvious peaks of Q<sub>4</sub> at -110 ppm and Q<sub>3</sub> at -101 ppm were seen for the pure silica aerogel (Curve (b)), which composed of typical Si(O<sub>1/2</sub>)<sub>4</sub> tetrahedral unit structures. The major structure also exhibited with Q<sub>4</sub> and Q<sub>3</sub> after APTES modification (Curve (a)), two small peaks belong to Q<sub>2</sub> and Q<sub>1</sub> are contributed by the little amount of unhydrolyzed Si-OC<sub>2</sub>H<sub>5</sub> groups on silica network. However, the new simultaneous appearances of amine propyl (Si-(CH<sub>2</sub>)<sub>3</sub>NH<sub>2</sub>) which labeled the strong peaks at -48.6 ppm, -55.2 ppm and -66.4 ppm corresponded to T<sub>1</sub>, T<sub>2</sub> and T<sub>3</sub> structure on the modified silica network (Curves (a)) suggested that the silica aerogel modifications took place rather completely. Compared to the pure silica aerogel (curve (d)), <sup>13</sup>C NMR spectra of the amine-modified silica aerogel (curve (c)) also showed new peaks at 9.5, 22.3 and 42.4 ppm representing the -(CH<sub>2</sub>)<sub>3</sub>NH<sub>2</sub> moiety. These new peaks were attributed to different carbon environments in the organo-silane as denoted as A, B and C showing the incorporation of amine groups. The results from NMR analysis and EDS element maps (Fig. S5) suggested the amine groups were uniformly distributed on surfaces of the amine-modified aerogel network.

In order to obtain more detailed quantitative information of chemical composition, XPS spectra of Si(2p), C(1s), N(1s) and O (1s) were tested and analyzed, the results are illustrated in Fig. 5 and summarized in Table 1. The wide scan XPS spectra of amine-modified aerogel showed a new peak of N (1s) peak at 399.3 eV compared to pure silica network, and Si (2s), Si (2p), C(1s) and O (1s) were observed (Fig. S3). The chemical compositions of Si-O<sub>4</sub> in Si(2p) as well as O-Si in O(1s) are from the pure silica network structure, while the new species of (C)-Si-O<sub>3</sub> in Si(2p), N-C in N (1s), C-Si and C-N in C(1s) indicated that the silica network are modified by APTES. As shown in Table 1, the amount of Si-O<sub>4</sub> and (C)-Si-O<sub>3</sub> for amine-modified silica aerogel is 27.1% and 72.9%, respectively, while that of C-Si and C-N in C(1s) are 25.2% and 16.9%, respectively. The amount of O-H (6.5% in Table 1) is contributed by the residual water on silica network.

### 3.3. CO<sub>2</sub> adsorption performances of the amine-modified silica aerogel

The CO<sub>2</sub> adsorption-desorption isotherms of pure silica aerogel and amine-modified xerogel/aerogel at 0 °C and 25 °C were presented at Fig. 6. It was found that the CO<sub>2</sub> adsorption isotherms and desorption isotherms of pure silica aerogel coincided with each other, which indicated that CO<sub>2</sub> adsorption on the pure silica aerogel was physical adsorption in nature and the CO<sub>2</sub> adsorption-desorption process is reversible. CO<sub>2</sub> adsorption capacity of the pure silica aerogel decreased with the increase in adsorption temperature, and the maximum adsorption capacity of the pure silica aerogel was only 0.5 mmol/g at 25 °C, indicating the adsorption of CO<sub>2</sub> on the pure silica aerogel could be an exothermic process and desorption becomes prominent with temperature increasing.

The amine-modified silica xerogel and aerogel showed obvious improvement of CO<sub>2</sub> adsorption capacity, which can be attributed to the more important role of chemical adsorption. The processes of CO<sub>2</sub> adsorption on the amine-modified silica xerogel and aerogel, which could be divided into two stages, are different from that of CO<sub>2</sub> adsorption on pure silica aerogel. First, the amount of CO<sub>2</sub> adsorption quickly increased at CO<sub>2</sub> partial pressure (P/P<sub>0</sub>) < 0.1, which might be resulted from the chemical interaction between CO<sub>2</sub> and the modified amine groups. At this stage, the CO<sub>2</sub> adsorption capacity is mainly controlled by adsorption temperature and available surface amine content. Then, the CO<sub>2</sub> adsorption capacity have a relatively slow improvement with an increase in CO<sub>2</sub> partial pressure at 0.1 < P/P<sub>0</sub> < 1, which mainly belongs to the physical adsorption of adsorbent. During the CO<sub>2</sub> desorption process, most

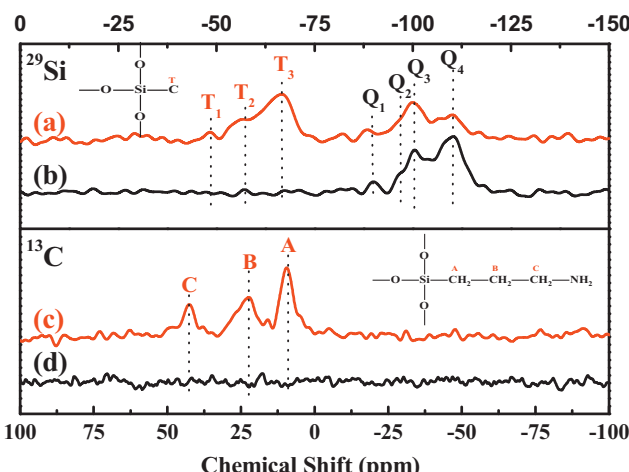
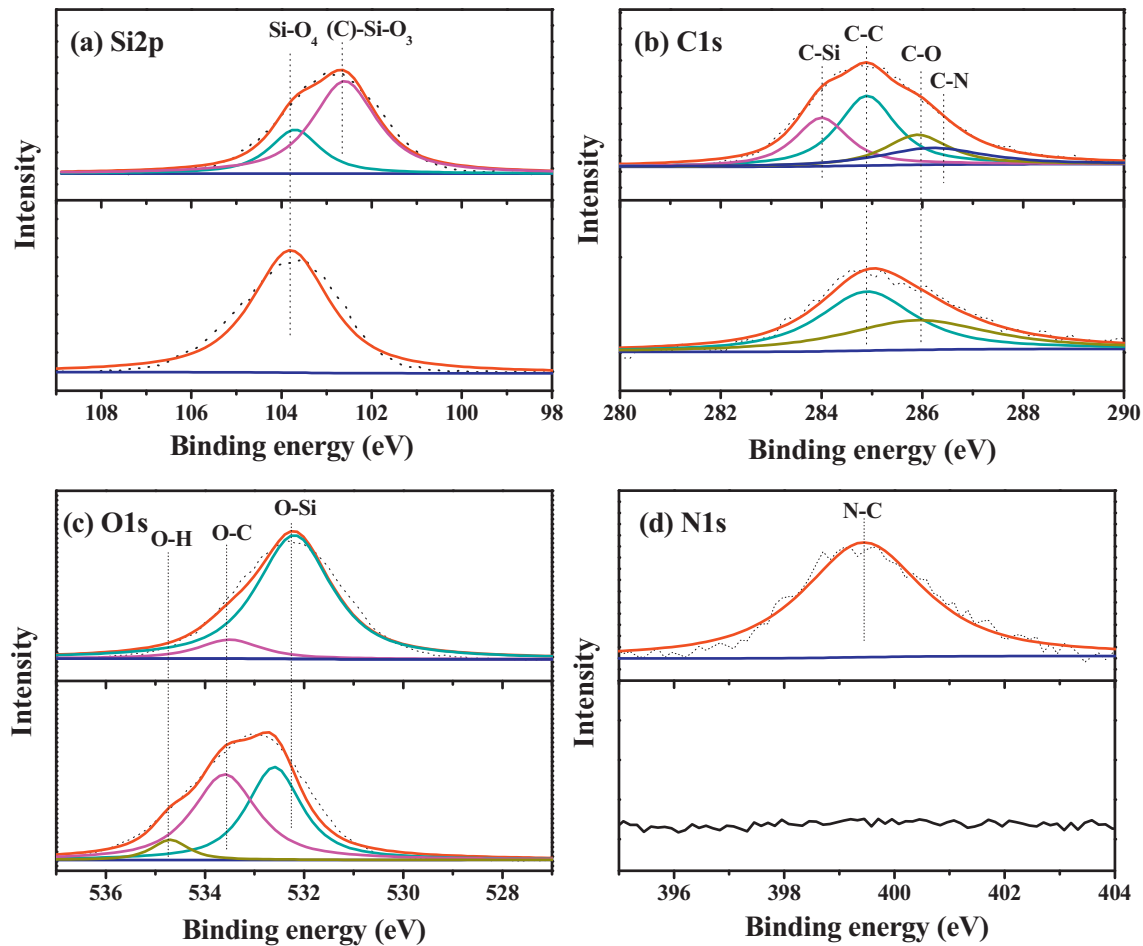


Fig. 4. <sup>29</sup>Si and <sup>13</sup>C NMR spectra of pure silica aerogel (curve b, curve d) and amine-modified silica aerogel (curve a, curve c).



**Fig. 5.** XPS spectra of (a) Si2p, (b) C1s, (c) O1s and (d) N1s for amine-modified silica aerogel (up curves) and pure aerogel (down curves).

**Table 1**  
Binding Energy and Relative Content of Si, C, N and O in Silica Aerogel and Amine-modified Silica Aerogel.

XPS	Chemical composition	Silica aerogel		Amine-modified silica aerogel	
		Binding Energy (eV)	Amount (%)	Binding Energy (eV)	Amount (%)
Si (2p)	Si-O <sub>4</sub> (C)-Si-O <sub>3</sub>	103.8	100	103.7 102.6	27.1 72.9
C (1s)	C-C C-O C-Si C-N	284.9 285.9	56.8 43.2	284.9 285.9 284.0 286.2	39.3 18.6 25.2 16.9
N (1s)	N-C			399.3	100
O (1s)	O-Si O-C O-H	532.6 533.6 534.7	44.8 48.7 6.5	532.2 533.5	88.8 11.2

of the adsorbed CO<sub>2</sub> is difficult to be released owing to high intermolecular forces between CO<sub>2</sub> and amine groups. The CO<sub>2</sub> adsorption isotherms on amine-modified silica xerogel/aerogel (Fig. 6b and c) showed similar results of higher CO<sub>2</sub> adsorption capacities at 25 °C than that at 0 °C. This may be because that at 25 °C, more sites are active for chemisorption and more CO<sub>2</sub> molecules diffuse into the particles to react with the active sites inside the silica particles, which is termed as a kinetically diffusion-controlled process. Consequently, the adsorption capacities were improved by the increased reaction rate at elevated temperatures. The porous properties of adsorbent are also important to improve the CO<sub>2</sub> adsorption capacity. As shown in Fig. 3, the pores of silica xerogel

seriously collapsed during ambient pressure drying, which decreases the available surface amine content and prevents the amine groups from reacting with CO<sub>2</sub> molecules. However, the high porosity and open pore volume of the amine-modified silica aerogel improved the available surface amine content, and the adsorption capacity of amine-modified silica aerogel was higher than 2.2 mmol/g at 25 °C.

In order to demonstrate a deeper insight into the nature of CO<sub>2</sub> adsorption onto the amine-modified silica aerogel, four adsorption equilibrium isotherm models have been used to fit the experimental data. Fig. S4 showed the Langmuir, Freundlich, Toth and Sips models, which was fit to the CO<sub>2</sub> adsorption equilibrium data.

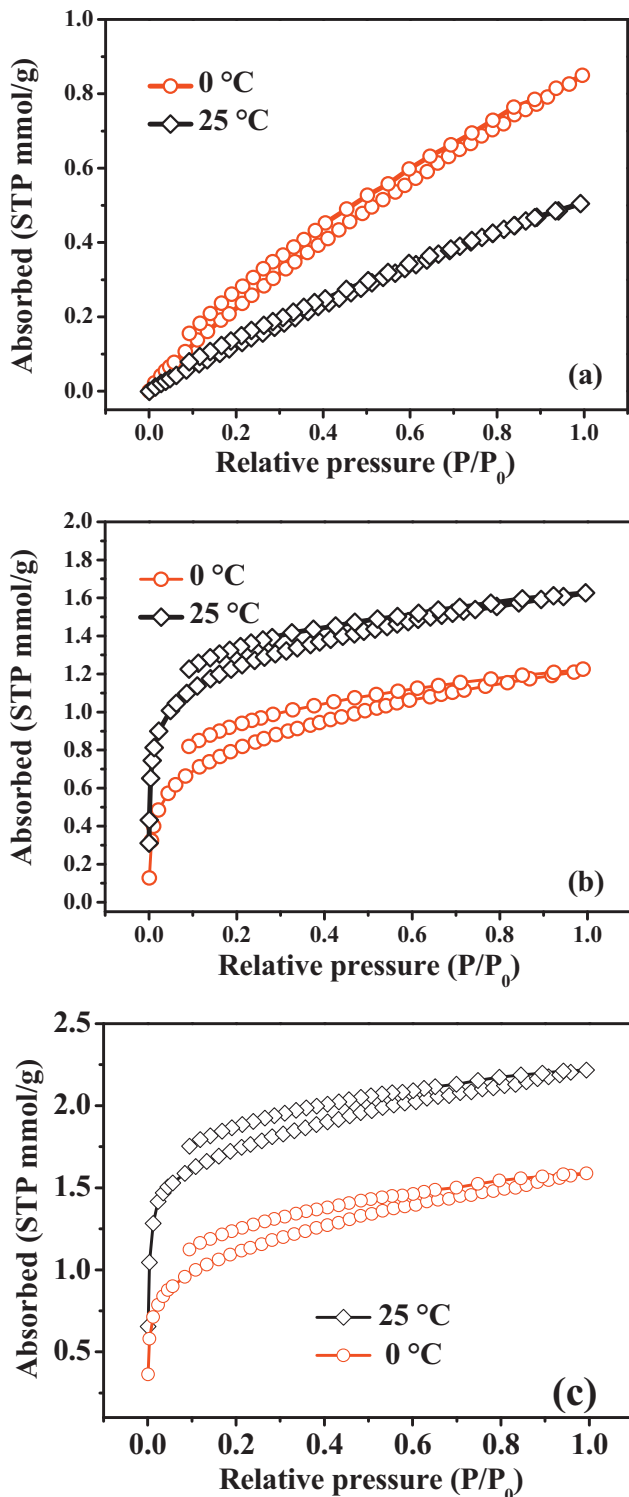


**Fig. 6.** CO<sub>2</sub> adsorption-desorption isotherms of: (a) pure silica aerogel, (b) amine-modified xerogel, and (c) amine-modified aerogel.

The hypothesis of Langmuir isotherm model is that monolayer adsorption occurs on the homogeneous adsorbent surface, while the Freundlich isotherm model is an empirical equation to describe multilayer adsorption on heterogeneous adsorbent surface. The Toth and Sips models are modified based on Langmuir and Freundlich models respectively. The parameter value of  $n$  in Sips model and  $t$  in Toth model can provide information of the nature

of adsorbent surface. The adsorbent is homogeneous if  $n$  (Sips parameter) and  $t$  (Toth parameter) near 1, on the other hand, the adsorbent is heterogeneity if  $n$  (Sips parameter)  $> 1$  and  $t$  (Toth parameter)  $< 1$ . It was observed that Toth and Sips isotherm models could describe the experimental data well. The fitted model parameters indicated that pure silica aerogel is homogeneous in nature, because of the value of  $n$  (Sips parameters) and  $t$  (Toth parameter) were near 1. In reality, it is expected that the two surface functional groups of siloxane linkage dipole and isolated silanol Si-OH/Si-OC<sub>2</sub>H<sub>5</sub> are randomly distributed on the periphery of the silica aerogel pores. The major interaction forces between CO<sub>2</sub> and surface functional groups of pure silica aerogel are due to dispersive force and hydrogen bond. Hence, it is assumed that all active sites on the pure aerogel network might possess a similar energy to adsorb CO<sub>2</sub>. However, it was found that the amine-modified silica aerogel exhibited obvious heterogeneity because of the value of  $n$  (Sips parameter)  $> 1$  and  $t$  (Toth parameter)  $< 1$ , which suggested the amines on the silica network had stronger chemisorption affinity towards CO<sub>2</sub> than the surface silanol group.

In addition to the adsorption isotherm study, the CO<sub>2</sub> adsorption performance of adsorbent can be also evaluated by exploring breakthrough curve of the dynamic adsorption process, which can offer advantage of determination of the dynamic adsorption capacities in practical application. The obtained CO<sub>2</sub> adsorption breakthrough curves of the adsorbents at 25 °C are presented in Fig. 7a, while the elemental composition and CO<sub>2</sub> adsorption capacities were illustrated in Table 2. The blank curve was

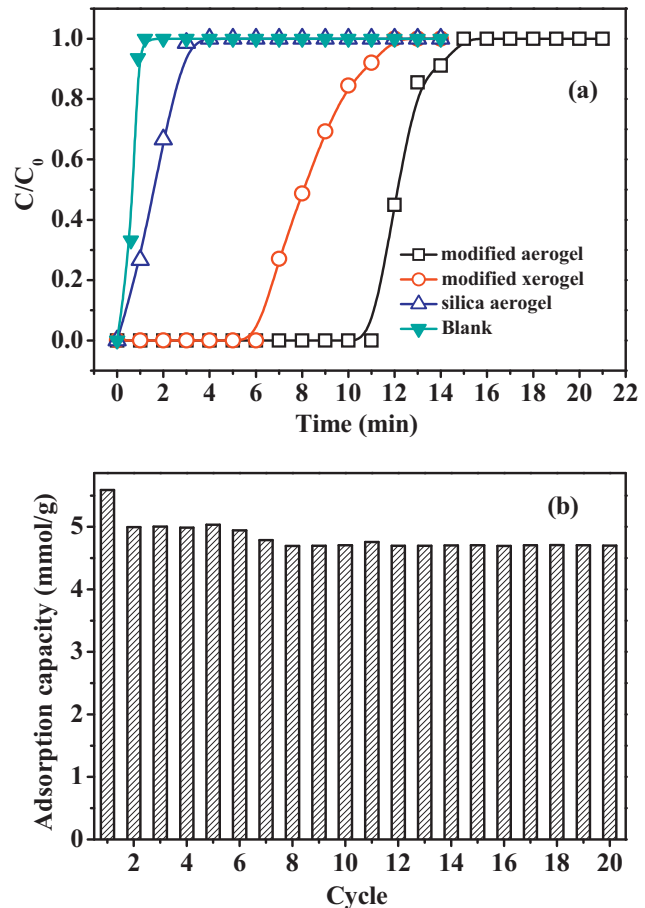


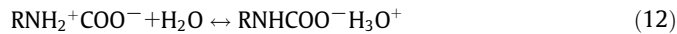
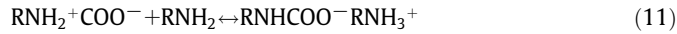
**Fig. 7.** (a) Breakthrough curves of dynamic adsorption of CO<sub>2</sub> on the pure silica aerogel, amine-modified silica xerogel/aerogel, and (b) cyclic adsorption capacity of CO<sub>2</sub> on the amine-modified silica aerogel. Experimental conditions: Mixed gas of CO<sub>2</sub>/N<sub>2</sub> with 10% CO<sub>2</sub> and 1% water vapor was used, the gas flow rate was maintained at 30 ml/min, and the temperature was controlled at 25 °C.

**Table 2**The element contents and CO<sub>2</sub> adsorption capacities of different adsorbents.

Adsorbents	Element contents			Amine contents (mmol/g)	CO <sub>2</sub> adsorption capacity (mmol/g)
	Carbon (wt%)	Carbon (mmol/g)	Nitrogen (wt%)		
Pure silica aerogel	1.38	1.15	0	0	0.43
Amine-modified silica xerogel	14.3	11.89	4.9	3.50	3.43
Amine-modified silica aerogel	13.8	11.48	4.8	3.42	5.59

measured when no adsorbent was in the reactor. All of the CO<sub>2</sub> adsorption capacities of the adsorbents were determined by the enclosed area between the blank curve and the curve with adsorbent. Elemental analyses of the amine-modified silica aerogel and xerogel are compared to that of the pure silica aerogel. The results showed that the amine-modified xerogel and aerogel have much higher carbon (>11%) and nitrogen (~5%) elemental content, which are derived from the methylene and amine groups of APTES. Due to the selective chemisorption of CO<sub>2</sub> on amine groups on the silica network surface, the amine-modified silica xerogel exhibited a high CO<sub>2</sub> adsorption capacity of 3.43 mmol/g (Fig. 7a), which is almost eight times higher than that of pure silica aerogel (0.43 mmol/g). The amine-modified silica aerogel exhibited the highest CO<sub>2</sub> adsorption capacity of 5.59 mmol/g, and the breakthrough time in dynamic adsorption curves was obviously prolonged to 10 min (Fig. 7a). This is because that the amine-modified silica aerogel prepared by supercritical drying reserved the excellent physical properties, such as high porosity and slit-shaped open pores, of which the surface amine groups could efficiently contact and react with CO<sub>2</sub> molecules.

The results demonstrated that the dynamic CO<sub>2</sub> adsorption capacity (5.59 mmol/g) of the amine-modified silica aerogel under humid mixed gas condition was much higher than the static adsorption capacity (2.2 mmol/g) under anhydrous mixed gas condition. Previous studies proposed, under unhydrous condition, CO<sub>2</sub> adsorption on amine adsorbent is by the formation of carbamate through a two-step zwitterion mechanism (Reactions (10) and (11)). The CO<sub>2</sub> firstly reacts with amine group to form a short-lived zwitterion. Then, the zwitterion was deprotonated by another amine group to form a stable ammonium carbamate under anhydrous condition. However, the zwitterion can be deprotonated and stabilized by water to form hydronium carbamate under humid condition (Reaction (12)). The addition of water vapor into the dynamic CO<sub>2</sub> adsorption system could cause the metastable behavior to vanish and that more amine molecules react with CO<sub>2</sub>, hence, dramatically increasing the CO<sub>2</sub> adsorption capacity of the amine-modified aerogel [29].



As shown in Fig. S7(a), the dynamic adsorption capacities of the amine-modified silica aerogel at 25 °C under anhydrous mixed gas and humid mixed gas with 1% water vapor conditions are 2.24 mmol/g and 5.59 mmol/g, respectively. The result further confirmed water could be beneficial to the CO<sub>2</sub> adsorption. On the other hand, the macropores especially for pores >100 nm are not detectable by the pore structure analyzer. The amine-modified silica aerogels have a large number of macropores, which could improve the dynamic CO<sub>2</sub> capacity [28].

To better understand the effect of temperature on the amine-modified silica aerogel performance, comparison experiments of

dynamic CO<sub>2</sub> adsorption capacities of the amine-modified silica aerogel at different temperature were carried out, and the results were shown Fig. S7(b). It can be seen that the influence of temperature on the dynamic CO<sub>2</sub> adsorption capacity of the amine-modified silica aerogel is insignificant at temperature ranging from 20 to 50 °C.

Cycle life is also a very important criterion to evaluate the performance of adsorbent. The cyclic CO<sub>2</sub> adsorption capacity of amine-modified silica aerogel was tested and presented in Fig. 7b. Compared to the first cycle, the CO<sub>2</sub> adsorption capacity of the amine-modified aerogel reduced by 10% in the second cycle, and afterwards remained almost unchanged. The amine-modified silica aerogel still showed good cyclic ability for the adsorption of carbon dioxide in the following cycles. Hence, the amine-modified silica aerogel showed good cyclic ability in CO<sub>2</sub> adsorption-desorption. The 10% decrease of adsorption capacity in the second cycle could be caused by desorption of adsorbed water on amine-modified silica network, which could lead to collapse of a bit of silica aerogel mesopores [30].

The temperature programmed desorption (TPD) of CO<sub>2</sub> on the amine-modified silica aerogel demonstrated the CO<sub>2</sub> desorption peak located at 80 °C, and desorption of CO<sub>2</sub> almost completed at 100 °C with a flow of 100 ml/min of purge N<sub>2</sub> gas (Fig. S8 in Supplementary Information). The flow rate of nitrogen would obviously affect the desorption peak. The TPD curves suggested the adsorbed CO<sub>2</sub> on the amine-modified aerogel could be quickly desorbed.

The comparisons of CO<sub>2</sub> adsorption capacities of the amine-modified aerogel prepared in this work with other reported amine-modified porous silica adsorbents are showed in Table 3. It can be seen that the amine-modified silica aerogel in this study has much higher CO<sub>2</sub> adsorption capacity than most of other porous amine-modified silica adsorbents reported, indicating the significant potential of the amine-modified silica aerogel as a CO<sub>2</sub> adsorbent.

**Table 3**Comparison of CO<sub>2</sub> adsorption capacities of the prepared amine-modified silica adsorbent with other reported data.

Adsorbent	Pressure (bar)	Temperature (°C)	Adsorption capacities (mmol/g)	References
SBA-12	1	25	1.04	[31]
MCM-41	1	25	1.15	[32]
MCM-48	0.05	25	1.02	[33]
Mesoporous silica	1	25	1.25	[16]
Silica gel	1	30	0.41	[34]
Silica xerogel	1	30	1.10	[35]
Silica xerogel	1	0/25	1.23/1.63	This work
Silica aerogel	1	25	1.2	[23]
Silica aerogel	1	25	1.92	[36]
Silica aerogel	1	25/50	2.0/1.2	[22]
Silica aerogel	1	0/25	1.59/2.22	this work
Silica aerogel	1	25	2.50 (humid)	[22]
Silica aerogel	1	25	5.55 (humid)	[28]
Silica aerogel	1	25	5.59 (humid)	This work

### 3.4. Adsorption and desorption mechanism analysis

In-situ DRIFTS study can indicate the concentration gradient change in the formed chemical species during  $\text{CO}_2$  adsorption or desorption process, which can provide information of the  $\text{CO}_2$  adsorption mechanism on amine-modified aerogel network.

In order to understand the process of  $\text{CO}_2$  captured by the amine-modified silica aerogel, DRIFTS absorbance spectra and normalized IR absorbance intensity profile of the amine-modified silica aerogel during  $\text{CO}_2$  adsorption process were measured, and the results were showed in Fig. 8a and d. It can be seen that several new bands appeared during  $\text{CO}_2$  adsorption. The bands at  $3423\text{ cm}^{-1}$  was assigned to N-H stretching vibrations, which could be caused by the N-H stretch of carbamate ( $-\text{NHCOO}^-$ ), the bands at  $3056\text{ cm}^{-1}$ ,  $2531\text{ cm}^{-1}$  and  $1635\text{ cm}^{-1}$  were assigned to primary ammonium ions species ( $\text{NH}^{3+}$ ), and the band at  $2184\text{ cm}^{-1}$  was

attributed to secondary ammonium ions species ( $\text{NH}^{2+}$ ). Furthermore, the bands in the ranges of  $1320\text{--}1567\text{ cm}^{-1}$  were attributed to carbamate species. All the above-mentioned bands could be possibly caused by the chemical adsorption of  $\text{CO}_2$  on the amine groups on aerogel network (Fig. 8a). The obvious bands at  $2360\text{ cm}^{-1}$  and  $2341\text{ cm}^{-1}$  were caused by gaseous or physically adsorbed  $\text{CO}_2$  on aerogel network.

During  $\text{CO}_2$  adsorption process, the peaks which assigned to carbamate species due to chemisorption were first appear in the spectra and followed by the appearance of physically adsorbed  $\text{CO}_2$  in  $2360\text{ cm}^{-1}$  and  $2341\text{ cm}^{-1}$ . It was found that the absorption bands at  $3056\text{ cm}^{-1}$ ,  $2531\text{ cm}^{-1}$ ,  $2184\text{ cm}^{-1}$  and  $1495\text{ cm}^{-1}$  began to appear in the spectra in 10 min and gradually increased during  $\text{CO}_2$  adsorption. It could be attributed to the fact that chemical adsorption of  $\text{CO}_2$  occurred on the aerogel network, implying that reaction kinetics of  $\text{CO}_2$  with amine groups on the aerogel network

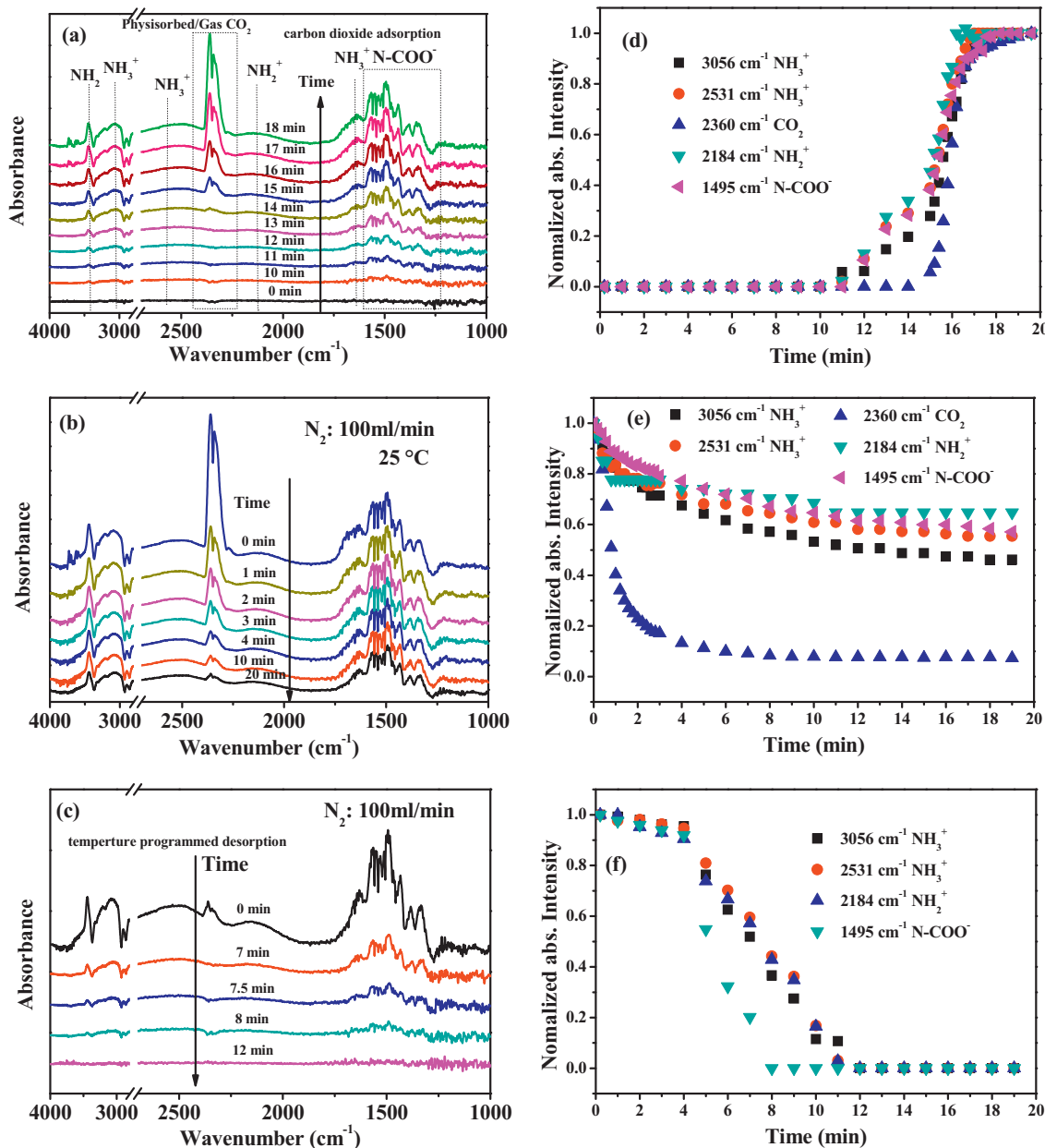


**Fig. 8.** DRIFTS mode IR absorbance spectra of amine-modified silica aerogel during: (a)  $\text{CO}_2$  adsorption process; (b)  $\text{CO}_2$  desorption process at  $25\text{ }^\circ\text{C}$ ; and (c) temperature programmed  $\text{CO}_2$  desorption; normalized IR absorbance intensity profiles of amine-modified silica aerogel during: (d)  $\text{CO}_2$  adsorption, (e)  $\text{CO}_2$  desorption at  $25\text{ }^\circ\text{C}$  and (f) temperature programmed  $\text{CO}_2$  desorption.

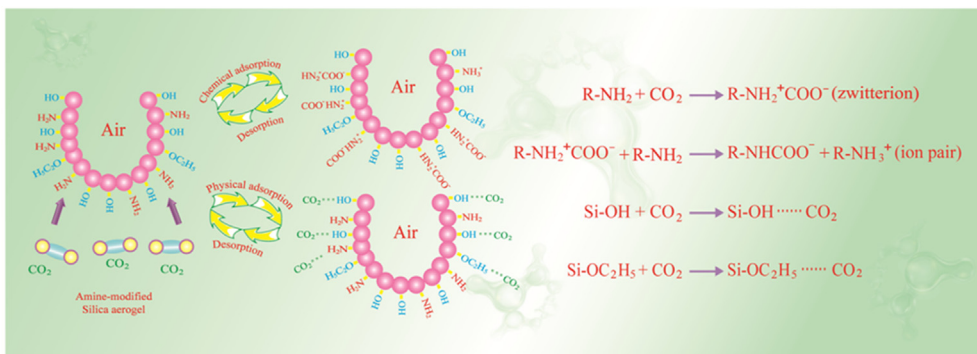


**Fig. 9.** Schematic mechanism of  $\text{CO}_2$  adsorption and desorption on the amine-modified silica aerogel.

is fast. Then, the absorption bands at  $2360\text{ cm}^{-1}$  and  $2341\text{ cm}^{-1}$  gradually appeared and increased, suggesting that chemical adsorption and physical adsorption of  $\text{CO}_2$  simultaneously occurred on the surface of aerogel network.

Fig. 8b and c show the DRIFTS absorbance spectra of amine-modified silica aerogel saturated with  $\text{CO}_2$  during the desorption process by  $\text{N}_2$  purge and TPD, respectively. The gaseous or physically adsorbed  $\text{CO}_2$  on aerogel network by weakly hydrogen bond was quickly removed by  $\text{N}_2$  purge, which was proved by the changes of band at  $2360\text{ cm}^{-1}$ . However, it was observed that the absorbance intensity of carbamate and ammonium ion on the aerogel network reduced slowly at  $25^\circ\text{C}$ , which can be considered as a strongly adsorbed species. The DRIFTS spectra of amine-modified silica aerogel during  $\text{CO}_2$  TPD process verified that the chemical adsorbed  $\text{CO}_2$  could be completely desorbed with increasing temperature. Desorption of chemically adsorbed  $\text{CO}_2$  from amine-modified silica aerogel will be accelerated in a higher desorption temperature to break the strong binding of ion pairs and zwitterions to  $-\text{NH}_2$  groups.

Based on the above analyses of  $\text{CO}_2$  adsorption and desorption isotherms, as well as the DRIFTS absorbance spectra of amine-modified silica aerogel during the adsorption and desorption process, the mechanisms of  $\text{CO}_2$  adsorption and desorption on the amine-modified silica aerogel are proposed and schematically shown in Fig. 9. On one hand, the majority of  $\text{CO}_2$  molecules are chemically adsorbed by reacting with  $-\text{NH}_2$  groups on the aerogel network to form carbamate type zwitterions at low  $\text{CO}_2$  partial pressure (Fig. 6c). On the other hand, partial of the  $\text{CO}_2$  were adsorbed by interacting with surface hydroxyl groups on the aerogel network through dispersive forces or hydrogen bonding at high  $\text{CO}_2$  partial pressure (Fig. 6c). During the  $\text{CO}_2$  desorption process, the physically adsorbed  $\text{CO}_2$  could be easily removed by  $\text{N}_2$  gas purge because of the weakness of physical adsorption force. However, the formed ammonium ions and carbamate species are tightly stabilized in low partial pressure of  $\text{CO}_2$ , which are proved by the need of higher temperature to convert these species back into amine groups during the  $\text{CO}_2$  desorption process.

#### 4. Conclusion

In summary, a transparent amine-modified silica aerogel with excellent physical properties was prepared by a facile co-precursor method. The amine-modification was easily achieved by APTES modification on the wet-gel network and kept the unique physical porosity of silica aerogel based on sol-gel growth mechanism and drying method. The highly selective adsorption of  $\text{CO}_2$  by the amine group enabled the amine-modified silica aerogel excellent adsorption performance. The maximum static and dynamic  $\text{CO}_2$  adsorption capacities of the amine-modified silica aerogel

were  $2.2\text{ mmol/g}$  and  $5.59\text{ mmol/g}$  under anhydrous and humid mixed gas conditions, respectively. The addition of water vapor is beneficial to the  $\text{CO}_2$  adsorption. The  $\text{CO}_2$  adsorption on the amine-modified silica aerogel is by the formation of carbamate through a two-step zwitterion mechanism. The amine-modified silica aerogel also showed good cyclic stability. This novel amine-modified aerogel could be applied as a promising adsorbent for  $\text{CO}_2$  capture.

#### Acknowledgements

The authors acknowledge financial support received from the National Natural Science Foundation of China (grant nos. of 51578525 and 5153000136), the China Postdoctoral Science Foundation (2015M571974), the Science and Technology Planning Project of Xiamen City (3502Z20162004), the Fujian Key Laboratory of Advanced Materials (Xiamen University), the Knowlegde Innovation Program of the Chineses Academy of Sciences (IUEQN201502) and Zhongke Tongde (Xiamen) I.O.T. Technology Co., Ltd.

#### References

- [1] M. Meinshausen, N. Meinshausen, W. Hare, S.C.B. Raper, K. Frieler, R. Knutti, D.J. Frame, M.R. Allen, *Nature* 458 (2009) 1158–1162.
- [2] D.J. Hofmann, J.H. Butler, P.P. Tans, *Atmos. Environ.* 43 (2009) 2084–2086.
- [3] L.B. Firth, N. Mieszkowska, R.C. Thompson, S.J. Hawkins, *Environ. Sci. Processes. Impacts.* 15 (2013) 1665–1670.
- [4] G.X. Zhao, X.B. Huang, X.X. Wang, X.K. Wang, *J. Mater. Chem. A* 5 (2017) 21625–21649.
- [5] G.T. Rochelle, *Science* 325 (2009) 1652–1654.
- [6] J. Wang, R. Krishna, T. Yang, *J. Mater. Chem. A* 4 (2016) 13957–13966.
- [7] Y. Belmabkhout, A. Sayari, *J. Am. Chem. Soc.* 132 (2010) 6312–6314.
- [8] Z. Rui, M. Anderson, Y. Li, Y.S. Lin, *J. Membr. Sci.* 417–418 (2012) 174–182.
- [9] M. Rana, K. Subramani, M. Sathish, U.K. Gautam, *Carbon* 114 (2017) 679–689.
- [10] H.Y. Zhao, X.N. Luo, H.J. Zhang, N.N. Sun, W. Wei, Y.H. Sun, *Greenh. Gases.* 8 (2018) 11–36.
- [11] R.Z. Chen, J.F. Yao, Q.F. Gu, S. Smeets, C. Baerlocher, H.X. Gu, D.R. Zhu, W. Morris, O.M. Yaghif, H.T. Wang, *Chem. Commun.* 49 (2013) 9500–9502.
- [12] B. Szczesniak, J. Choma, M. Jaroniec, *J. Colloid Interface Sci.* 514 (2018) 801–813.
- [13] R. Serna-Guerrero, A. Sayari, *Chem. Eng. J.* 161 (2010) 182–190.
- [14] C. Chen, N.J. Feng, Q.R. Guo, Z. Li, X. Li, J. Ding, L. Wang, H. Wan, G.F. Guan, *J. Colloid Interface Sci.* 513 (2018) 891–902.
- [15] G.P. Knowles, J.V. Graham, S.W. Delaney, A.L. Chaffee, *Fuel. Process. Technol.* 86 (2005) 1435–1448.
- [16] S.N. Kim, W.J. Son, J.S. Choi, W.S. Ahn, *Micro. Meso. Mater.* 115 (2008) 497–503.
- [17] S.S. Kistler, *Nature* 127 (1931), 741.
- [18] N. Husing, U. Schubert, *Angew. Chem. Int. Ed.* 37 (1998) 23–45.
- [19] M. Koebel, A. Rigacci, P. Achard, *J. Sol-Gel Sci. Technol.* 63 (2012) 315–339.
- [20] A.C. Pierre, G.M. Pajonk, *Chem. Rev.* 102 (2002) 4243–4265.
- [21] S. Yun, H.J. Luo, Y.F. Gao, *J. Mater. Chem. A* 3 (2015) 3390–3398.
- [22] S. Cui, W. Cheng, X. Shen, M. Fan, A. Russell, Z. Wu, X. Yi, *Energy. Environ. Sci.* 4 (2011) 2070–2074.
- [23] N.N. Linneen, R. Pfeffer, Y.S. Lin, *Chem. Eng. J.* 254 (2014) 190–197.
- [24] L. Li, B. Yalcin, B.N. Nguyen, M.A.B. Meador, M. Cakmak, *ACS Appl. Mater. Interface* 1 (2009) 2491–2501.
- [25] J.P. Randall, M.A.B. Meador, S.C. Jana, *J. Mater. Chem. A* 1 (2013) 6642–6652.

- [26] S. Mulik, C. Sotiriou-Leventis, G. Churu, H. Lu, N. Leventis, *Chem. Mater.* 20 (2008) 5035–5046.
- [27] M.A.B. Meador, E.F. Fabrizio, F. Ilhan, A. Dass, G. Zhang, P. Vassilaras, J.C. Johnston, N. Leventis, *Chem. Mater.* 17 (2005) 1085–1098.
- [28] Y. Kong, G.D. Jiang, M.H. Fan, X.D. Shen, S. Cui, A.G. Russell, *Chem. Commun.* 50 (2014) 12158–12161.
- [29] K.J. Li, J.D. Kress, D.S. Mebane, *J. Phys. Chem. C* 120 (2016) 23683–23691.
- [30] D.A. Bostain, J.S. Brenizer, P.D. Norris, *Res. Nondestruct. Eval.* 14 (2002) 47–57.
- [31] Y.G. Ko, S.S. Shin, U.S. Choi, *J. Colloid Interface Sci.* 361 (2011) 594–602.
- [32] L. Wang, R.T. Yang, *J. Phys. Chem. C* 115 (2011) 21264–21272.
- [33] M. Gil, I. Tiscornia, O. Lglesia, R. Mallada, J. Santamaría, *Chem. Eng. J.* 175 (2011) 291–297.
- [34] O. Leal, C. Bolivar, C. Ovalles, J.J. Garcia, Y. spidel, *Inorg. Chim. Acta* 240 (1995) 183–189.
- [35] H.Y. Huang, R.T. Yang, D. Chinn, C.L. Munson, *Ind. Eng. Chem. Res.* 42 (2003) 2427–2433.
- [36] K.A.S. Abhilash, T.R. Deepthi, A. Sadhana, K.G. Benny, *ACS Appl. Mater. Interfaces* 7 (2015) 17969–17976.